Annual Review of Earth and Planetary Sciences

Superrotation on Venus, on Titan, and Elsewhere

Peter L. Read[1] and Sebastien Lebonnois[2]

[1]Clarendon Laboratory, Department of Physics, University of Oxford, Oxford OX1 3PU, United Kingdom; email: peter.read@physics.ox.ac.uk

[2]Laboratoire de Météorologie Dynamique (LMD/IPSL), Sorbonne Universités, UPMC Univ Paris 06, ENS, PSL Research University, Ecole Polytechnique, Université Paris Saclay, CNRS, 75000 Paris, France

Annu. Rev. Earth Planet. Sci. 2018. 46:175–202

First published as a Review in Advance on March 14, 2018

The *Annual Review of Earth and Planetary Sciences* is online at earth.annualreviews.org

https://doi.org/10.1146/annurev-earth-082517-010137

Keywords

atmospheres, dynamics, waves, Hadley circulation, Venus, Titan

Abstract

The superrotation of the atmospheres of Venus and Titan has puzzled dynamicists for many years and seems to put these planets in a very different dynamical regime from most other planets. In this review, we consider how to define superrotation objectively and explore the constraints that determine its occurrence. Atmospheric superrotation also occurs elsewhere in the Solar System and beyond, and we compare Venus and Titan with Earth and other planets for which wind estimates are available. The extreme superrotation on Venus and Titan poses some difficult challenges for numerical models of atmospheric circulation, much more difficult than for more rapidly rotating planets such as Earth or Mars. We consider mechanisms for generating and maintaining a superrotating state, all of which involve a global meridional overturning circulation. The role of nonaxisymmetric eddies is crucial, however, but the detailed mechanisms may differ between Venus, Titan, and other planets.

1. INTRODUCTION

One of the most remarkable features of the atmosphere of Venus, which has been observed for many decades but remains difficult to explain, is its global and local superrotation. This manifests itself in various ways, most notably in cloud structures that move rapidly around the planet in a direction parallel to the equator. The cloud markings, which appear with high contrast through an ultraviolet filter, have their origin at heights 60 to 70 km above the surface (where the pressure is on the order of 100 hPa) and travel around the equator in 4 to 5 days, corresponding to speeds near 100 m/s. This corresponds to an angular velocity about Venus's rotation axis that is more than 50 times faster than the rotation rate of the surface below. Measurements of the winds below the clouds (**Figure 1*a***; Counselman et al. 1980) and calculations of the winds above the cloud tops (from temperature data) show that the zonal wind speed declines at higher and lower levels, reaching values near zero at about 100 km and near the surface.

Direct measurements of the winds 1 m or so above the surface by the Russian landers Venera 9 and 10 found velocities of ≤1 m/s. Tracking of the Pioneer and Venera landers during their descent showed that there is a steady decrease with height from the 100 m/s or so observed in the ultraviolet markings near the cloud tops. Earth-based observers had earlier shown, by the measurement of Doppler-shifted emission lines from atmospheric gases, that the cloud-tracked winds do, in fact, apply to mass motions, rather than to the phase speed of waves or other coherent patterns, as had also been suggested (e.g., Kouyama et al. 2013).

When the Voyager missions first observed Titan's hazy atmosphere, superrotation was also suspected, and some indirect indications were obtained from available observations even though cloud tracking was not possible (Flasar et al. 1981). Large stratospheric zonal winds (on the order of 200 m/s) were also inferred from Earth-based observations. Superrotation was confirmed by

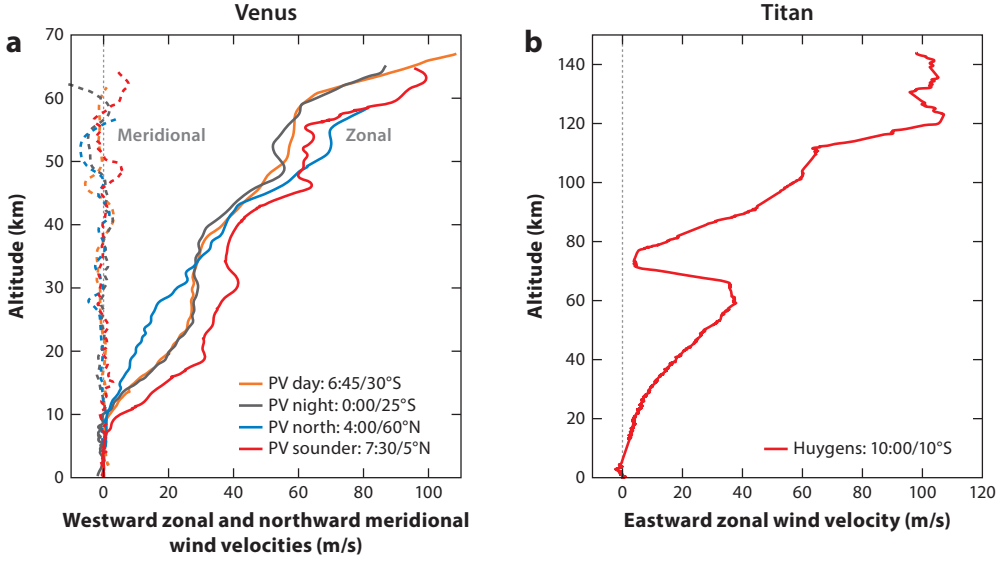

Figure 1

(*a*) Profiles of the zonal (east-to-west; *solid lines*) and meridional (south-to-north; *dashed lines*) wind on Venus as measured by tracking the Pioneer Venus (PV) entry probes. Data from Counselman et al. (1980). Note the suggestion of global layering, which has been interpreted as suggesting stacked Hadley circulation cells of considerable latitudinal extent. Local time and latitude of entry are indicated in the legend. (*b*) Profile of the zonal (west-to-east) wind on Titan, as measured by tracking the Huygens probe during its descent. Data from Bird et al. (2005).

in situ measurements with the Huygens probe (**Figure 1*b***; Bird et al. 2005). This makes Venus and Titan unique in the Solar System, as far as atmospheric dynamics are concerned, with zonal winds that are in cyclostrophic balance for which centrifugal accelerations ($u^2 \tan\phi/a$) balance horizontal pressure gradients (Leovy 1973) instead of Coriolis accelerations ($\mathbf{\Omega} \times u$) as on Earth and other rapidly rotating planets.

By combining the approximated meridional momentum equation for cyclostrophic balance with equations for hydrostatic balance and the ideal gas law, a further equation can be derived for the vertical derivative of u. In pressure coordinates, this becomes

$$\frac{\partial u^2}{\partial \zeta} = -\frac{R}{\tan\phi}\left(\frac{\partial T}{\partial \phi}\right)_p, \qquad 1.$$

where $\zeta = \ln(p/p_0)$ and p_0 is a reference pressure, and is referred to as the cyclostrophic thermal wind equation. Insofar as cyclostrophic balance is approximately satisfied by the flow, given a latitudinal profile of $\overline{u}(\phi)$ at a particular pressure level and measurements of temperature as a function of height and latitude, Equation 1 can be integrated upward to recover the complete field of $\overline{u}$ in ζ and ϕ (e.g., see Mendonça et al. 2012). This superrotation of Venus's and Titan's atmospheres is perhaps the most remarkable feature of their dynamical behavior, but how should we define superrotation in a quantitative manner, and why is it so remarkable?

1.1. Angular Momentum and Hide's Theorems

In some branches of geophysics it has been customary to define superrotation in terms of an excess of angular velocity compared with the bulk of the planet: for the rotation of Earth's inner core relative to the rest of the planet (e.g., Glatzmaier & Roberts 1996, Livermore et al. 2013) or for the mean angular velocity of the upper atmosphere (thermosphere) relative to the solid Earth (e.g., King-Hele 1964). For the atmosphere, however, it has been more common to quantify superrotation in terms of atmospheric angular momentum (e.g., Hide 1969, Read 1986), mainly because this is a more tangible physical quantity than angular velocity that may be materially conserved under certain circumstances. In any atmospheric circulation system the flow must everywhere satisfy certain key conservation principles in relation to energy, momentum, and angular momentum. The latter two quantities are strictly vectors, but in the case of angular momentum, the axial component (per unit mass) may be conserved under certain circumstances (e.g., Hide 1969, Read 1986).

We consider the axial component of specific absolute angular momentum, m, defined in spherical polar coordinates as

$$m = a\cos\phi(\Omega a\cos\phi + u). \qquad 2.$$

This quantity satisfies an important conservation principle in axisymmetric flow in the absence of external torques, which leads to two powerful theorems that allow us to define and quantify both global and local superrotation in a most insightful way.

1.1.1. Hide's theorem I. With the definition of m in Equation 2, the zonal equation of motion for axisymmetric flow implies that m is conserved following the motion in the meridional (ϕ, z) plane, meaning that specific axial angular momentum contained in rings of fluid aligned along latitude circles behaves like a materially conserved tracer. Once a ring of fluid has been initialized with a certain value of m, there is no means of changing it in the absence of friction, body torques, or nonaxisymmetric processes.

This suggests a way to define nondimensional measures of both local superrotation and global superrotation in relation to the ratio between the observed atmospheric angular momentum and

the value it would take in solid body corotation with the underlying planet. Indices of this form representing the ratio of total angular momentum to solid body rotation were proposed in several studies (e.g., Del Genio & Zhou 1996, Newman et al. 2011). Such indices take the value of unity in the case of solid body rotation, whereas Read (1986) proposed indices that compared the relative angular momentum excess with solid body rotation in the forms

$$s = \frac{m}{\Omega a^2} - 1, \qquad 3.$$

$$S_m = \frac{\iiint \rho m \, \mathrm{d}V}{\iiint \rho \Omega a^2 \cos^2 \phi \, \mathrm{d}V} - 1, \qquad 4.$$

where $\mathrm{d}V$ is an element of volume and S_m represents the mass-weighted global superrotation. Thus, $s \leq 0$ and $S_m = 0$ for any flow in solid body rotation with the underlying surface. S_m or s can also be regarded as the quotient of a mean zonal velocity, U, and Ωa and hence shares some characteristics of a zonal Rossby number (e.g., see Read 1986).

For a frictionless, axisymmetric system without external body torques, therefore, both s and S (or S_m) can never exceed zero without the need to invoke rather special initial conditions. This was a result first discussed in this context by Hide (1969) and is sometimes referred to as Hide's (first) theorem (e.g., Read 1986). It can be clearly illustrated in numerical simulations where care is taken to minimize the effects of internal numerical diffusion. **Figure 2** shows two examples, taken from the work of Mitchell & Vallis (2010), that illustrate and contrast the resulting flows when eddy–zonal flow interactions are suppressed (**Figure 2*b***) to those with fully three-dimensional eddies present. The two-dimensional flow spins up high-latitude prograde jets (for reasons discussed more fully below) but with essentially no zonal flow over the equator. With resolved eddies, however, the equator is brought into near–solid body rotation with higher latitudes (**Figure 2*a***) because of eddy fluxes of angular momentum.

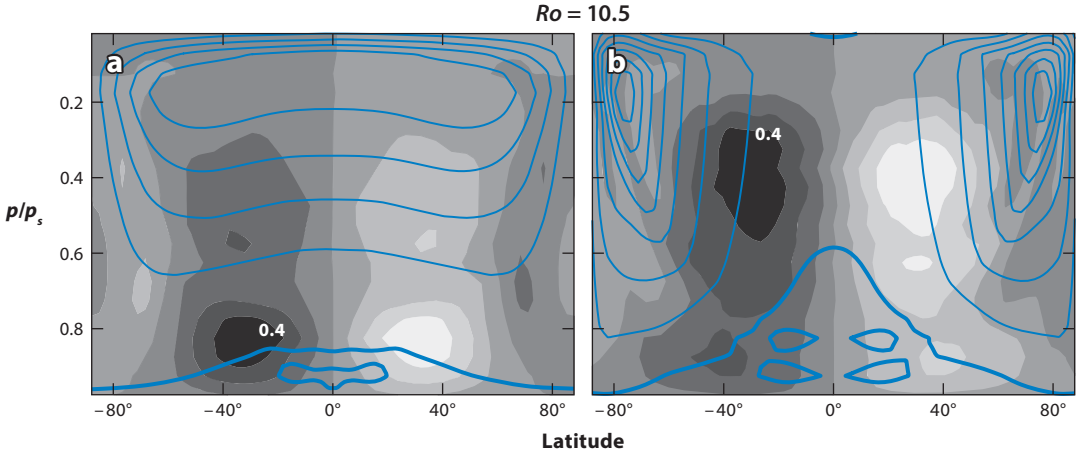

Figure 2

Contour maps of zonal-mean zonal flow and meridional stream function for the equilibrated flow in a slowly rotating atmospheric simulation (*a*) in a fully three-dimensional simulation and (*b*) in a two-dimensional, axisymmetric simulation under the same thermal forcing and boundary conditions. Adapted with permission from the results of simulations by Mitchell & Vallis (2010). Solid contours represent the zonal velocity and shaded contours the meridional mass stream function; p is the pressure, shown on the vertical axis relative to the surface pressure p_s.

1.1.2. Hide's theorem II. When nonaxisymmetric eddies (or viscous friction) are present, these arguments can be further generalized (Schneider 1977, Held & Hou 1980), based on the supposed properties of angular momentum transfer by an eddy viscosity in the presence of a local maximum of m. Thus, steady, prograde equatorial flow cannot occur, even in a viscous fluid, unless the effective eddy viscous diffusion coefficient, ν, is negative (thereby implying an effect obtainable only by nonaxisymmetric processes (e.g., see Starr 1968). This is because

$$\int\int \overline{\mathbf{F}} \cdot \mathrm{d}\mathbf{n} = 0, \qquad 5.$$

evaluated around a closed contour of m, where $\overline{\mathbf{F}}$ represents either the viscous flux or the zonally averaged eddy flux of angular momentum in the meridional plane. Excluding the trivial case, this implies that $\overline{\mathbf{F}}$ must either be everywhere parallel to the m contour or have components somewhere that act against the gradient of $\overline{m}$. A clearer statement of Hide's (second) theorem might then be that an axisymmetric atmosphere cannot superrotate at the equator if small-scale mixing of angular momentum is everywhere downgradient (see Section 4). This is sometimes quoted by itself as an argument that eddies are necessary for superrotation, although the situation in reality is somewhat more subtle. While eddies can act spontaneously to transfer angular momentum upgradient, either in the horizontal or in the vertical direction, such transfers can also occur in principle due to molecular viscosity (e.g., Read 1986), which acts in a Newtonian fluid to mix momentum toward a state of uniform angular velocity. In practice, however, molecular viscosity coefficients of gases are far too small to sustain an equatorward diffusive flux of angular momentum large enough to balance the advection of m by thermally direct meridional circulations without impossibly large horizontal shears. Eddies are much more efficient at effecting this transfer than is molecular viscosity, and various model simulation studies (e.g., Lee et al. 2005, Lebonnois et al. 2010) have shown that eddy momentum transfers are able to balance angular momentum transport by meridional circulations and thereby maintain a steady superrotation with much weaker shear in the zonal flow.

1.2. Where Is Superrotation Observed?

Although the principal focus of this article is on the atmospheres of Venus and Titan, it is of interest to consider other contexts where either local or global superrotation, as defined in Equations 3 and 4, is observed.

In the atmosphere of Earth itself, the zonal-mean zonal winds are typically eastward (prograde[1]) at middle latitudes but westward (retrograde) in the tropics, at least in the troposphere (e.g., Schneider 2006). Since the maximum absolute angular momentum in an atmosphere in solid body rotation is found at the equator, this suggests that local superrotation (indicated by $s > 0$ in Equation 3) is likely to be rare on Earth, at least in the zonal mean. This is borne out in observations, as can be seen, for example, in **Figure 3*a***. This plot was derived from a time series of daily values of atmospheric angular momentum from 1979 to 2006, computed within a latitude band between $+2.5°$ and $-2.5°$ by integrating over area and in pressure (mass-weighted) from 1,000 to 100 hPa. An estimate of the local superrotation index, s, was obtained by normalizing by $\rho\Omega a^2$, also integrated over the same area and pressure range. The results show s to undergo an annual oscillation but to remain negative almost all the time, with a mean value $s \simeq -0.007 \pm 0.0026$.

In the stratosphere at altitudes above 100 hPa, however, the zonal wind is dominated by the eddy-driven Quasi-Biennial Oscillation (see Baldwin et al. 2001), in which the wind direction

[1]The term prograde is taken hereafter to mean in the same sense as the rotation of the solid planet.

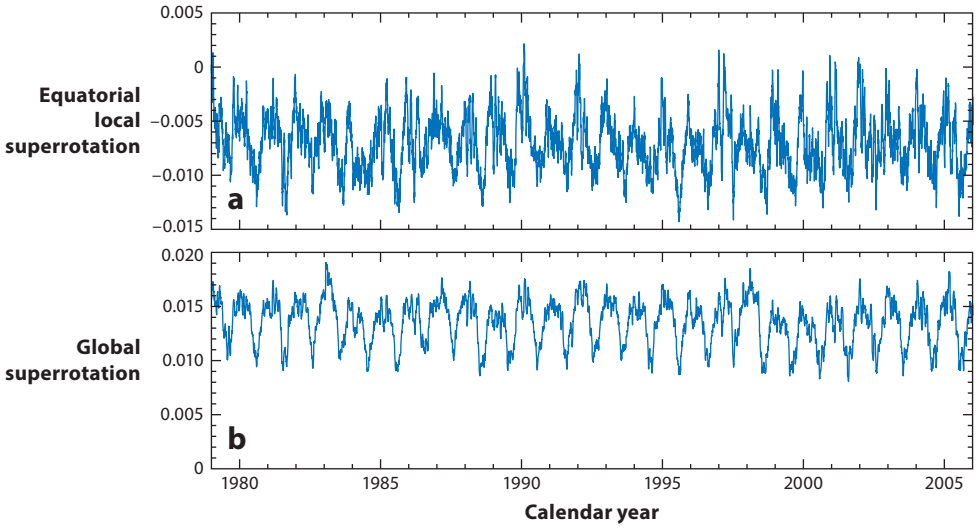

Figure 3

Time series of (*a*) local superrotation index s at the equator of Earth and (*b*) mass-weighted global superrotation index S_m as a function of time during the years 1979 to 2006 from the zonal-mean, vertically and area-integrated angular momentum statistics computed from National Centers for Environmental Prediction reanalyses by the Special Bureau for the Atmosphere at Atmospheric and Environmental Research. The data for panel *a* shown here are for the equatorial latitude band between +2.5° and −2.5°.

alternates between eastward and westward phases on a repeating timescale of around 28 months. This would suggest that s can be significantly greater than zero at these altitudes during the eastward phase, with wind speeds up to 20 m/s and a corresponding value for $s \simeq 0.04$. Global superrotation indices, on the other hand, are typically positive more or less all the time, indicating a general tendency for Earth's atmosphere to superrotate weakly. **Figure 3*b*** shows a corresponding time series of S_m, computed from the same data set as for **Figure 3*a*** but integrated over the whole planet and normalized by $M_{0m} = 8\pi\Omega a^4 p_s/(3g)$, the total angular momentum of an equivalent atmosphere in solid body rotation with the underlying planet (where p_s is the mean surface pressure, taken to be 1.013×10^5 Pa, and g the acceleration due to gravity). This quantity also shows a strong annual oscillation with a mean value of 0.0135 ± 0.002, consistent with a small Rossby number for a rapidly rotating planet like Earth.

The atmospheric circulation of Mars is similar in many respects to that of Earth, with horizontal winds in approximate geostrophic balance and the zonal flow dominated by seasonal midlatitude eastward jets (e.g., Read & Lewis 2004, Barnes et al. 2017). Near the equator, however, the mean zonal flow is more typically westward, much as is seen on Earth, except within around 10 km of the surface. The global superrotation, S_m, is estimated to be around three times that of Earth at $\simeq$0.045 (Lewis & Read 2003), though it probably fluctuates on seasonal timescales and with varying dust loading in the atmosphere. It is particularly noteworthy, however, that S_m appears to increase only slowly with dust loading [mainly associated with strengthening midlatitude zonal winds as thermal gradients increase (Lewis & Read 2003)]. The local superrotation, however, becomes significantly positive in the lowest 1–2 scale heights, at least in numerical model simulations, reaching values $\simeq$0.16 during very dusty seasons (Lewis & Read 2003). This appears to be associated with the interaction of the diurnal solar heating cycle with regions of thick suspended dust, leading to strong local heating and the excitation of an enhanced diurnal tide. Such a nonaxisymmetric tide

seems capable of driving relatively strong, rectified zonal flows that can be in excess of 30 m/s on the equator, around 1 scale height above the surface.

The gas giant planets, Jupiter and Saturn, also appear to exhibit strong local superrotation at the level of the visible cloud tops. Both planets have strong eastward zonal jets on their equators, with wind speeds around 60 and 430 m/s, respectively, on Jupiter and Saturn (e.g., Flasar 1986, Del Genio et al. 2009) but with the possibility of zonal winds exceeding 140 m/s in Jupiter's stratosphere (Flasar et al. 2004). Given their planetary radii and respective System III[2] rotation rates, this would suggest that the range of s on Jupiter is 0.005–0.011, whereas on Saturn the range is closer to 0.035–0.045. In contrast, the ice giant planets, Uranus and Neptune, appear to subrotate at their equators, with zonal winds measured respectively at around −80 and −400 m/s (e.g., Sromovsky & Fry 1993, Hammel et al. 2005). This would suggest maximum values for s at their cloud tops of around −0.03 and −0.15, respectively. Not much can be said at this stage about the global superrotation of any of these planets, since there is little information on the atmospheric flow beneath the visible cloud tops and atmospheric models have not yet been able to simulate their interior circulation with any degree of certainty. However, this situation may change soon for Jupiter and Saturn because of measurements of the gravity harmonics from the Juno and Cassini missions.

Gas giant planets are not limited solely to the Solar System but are frequently found around other low-mass stars, mainly in the form of close-in Hot Jupiters (e.g., Showman et al. 2010 and references therein). Zonal winds have recently been inferred for two examples of such objects, HD 189733b and HD 209458b, from observations (Snellen et al. 2010, Louden & Wheatley 2015) and from model simulations (e.g., Showman et al. 2010 and references therein) with prograde values of up to 2.4 km/s. These planets orbit so close to their parent stars that their rotation is almost certainly tidally locked to their orbit, indicating rotation periods of just a few Earth days. Given these rotation periods, the implied equatorial values of s are $\sim$1, suggesting that they are relatively slow rotators. In this case, however, numerical circulation models suggest that the strong zonal superrotation in these atmospheres is induced by wave processes driven by the extreme contrast in day-night stellar radiative heating.

Pluto and the icy moon of Neptune, Triton, also harbor significant atmospheres, albeit very tenuous, optically thin, and relatively shallow. Although there are no direct observations of winds so far, their atmospheric circulations have been modeled in three dimensions in some detail (e.g., Zalucha & Michaels 2013, Forget et al. 2017). Model results vary somewhat in their predictions, but equatorial zonal winds of 5–15 m/s were obtained, which, together with their relatively slow rotation rates, imply superrotation indices $\lesssim O(1)$ (see **Table 1**).

Finally, for completeness, we also include in **Table 1** values obtained for Venus and Titan (see Mendonça & Read 2016 for Venus). The basis for obtaining these values from combinations of direct observations and numerical models is reviewed in the following sections, but the clear message is that both of these planets stand in a class of their own when it comes to superrotation, as defined in Section 1.1.1 above. Peak values of local superrotation, s, are at least an order of magnitude greater even than for the Hot Jupiters discussed above, and 2–3 orders of magnitude larger than for Earth. Even the global superrotation, S_m, is at least $O(1)$ for Titan and nearly 10 times larger in the case of Venus, indicating that these atmospheres have the capacity to store massive amounts of angular momentum compared to what they would have in corotation with the underlying planet. It is this remarkable feature of both of these atmospheres that has proved extremely challenging to explain for many years.

[2]This is the reference frame of the planetary magnetic field, assumed to represent the rotation of the deep interior.

Table 1 Superrotation indices for Solar System and extrasolar atmospheres

Planet	a (km)	Ω (s^{-1})	$\overline{u}$ (m/s)	s_{max}	S_m
Earth	6,371	7.272×10^{-5}	−20–20	−0.015–0.04	0.0135 ± 0.002
Mars	3,396	7.088×10^{-5}	30	0.16	0.04
Jupiter	69,911	1.757×10^{-4}	60–140	0.005–0.011	—
Saturn	58,232	1.6378×10^{-4}	350–430	0.035–0.045	—
Uranus	25,562	1.012×10^{-4}	−80	−0.03	—
Neptune	24,622	1.083×10^{-4}	−400	−0.15	—
Pluto	1,152	1.139×10^{-5}	10–15	0.76–1.1	—
Triton	1,353	1.237×10^{-5}	5–10	0.3–0.6	—
HD 189733b	79,500	3.28×10^{-5}	2,400	0.93	—
HD 209458b	94,380	2.063×10^{-5}	1,940	1.00	—
Titan	2,576	4.559×10^{-6}	100–180	8.5–15	2
Venus	6,052	2.992×10^{-7}	100–120	55–65	7.7

2. MEASUREMENTS OF SUPERROTATION ON VENUS AND TITAN

2.1. Techniques

Measuring the wind field in the atmosphere of a planet is not an easy task. Several techniques may be used, either in situ or from remote sensing. The displacement of a probe moving along the flow can be tracked to measure the wind speed. An anemometer on a fixed probe on the surface can also give a local measurement of the surface wind. However, these in situ measurements are always very limited in time and space and give only a partial view of the wind field. Remote sensing techniques can provide more global views of the wind field. When contrast features are present due to differences in the abundance of cloud or dust particles, the hypothesis that these particles are moving with the flow yields an estimation of the wind speed through the measurement of the displacement of these contrasts between two images. This provides a horizontal wind field at the altitude where these contrasts are measured. However, caution must be taken when these contrasts are associated with wave activity, as they may be indicative of the phase velocity of the waves rather than the actual background wind speed. When emission or absorption lines are observed in the spectrum, the Doppler shift of these lines can be used to deduce the air velocity along the line of sight, at the altitude where the spectral line is formed. Temperature fields deduced from spectra inversion can also be used to deduce the zonal wind field, through the use of the gradient wind equation. This yields a relation between the latitudinal gradient of the temperature and the vertical gradient of the zonal wind (see Equation 1). Through observation of the structure of stellar occultation lightcurves made in several locations on Earth, information on winds can also be retrieved. The inversion of these lightcurves yields the shape of the density field in the atmosphere, from which the zonal wind velocity can be inferred. This technique, however, does not give access to the direction of the zonal wind velocity.

2.2. Superrotation on Venus

The thick cloud layer completely covering Venus provides an efficient way to measure the wind field. Depending on the wavelength, the altitude at which the cloud contrasts are observed is different. On the day side, the reflected sunlight shows contrasts in ultraviolet at the cloud top, at altitudes around 65–70 km, as well as for near-infrared wavelengths (950–980 nm), sensing

altitudes around 60 km. On the night side, radiation coming from the deep atmosphere through infrared windows (1.7 and 2.3 μm) provides contrast due to the cloud opacity in the lower cloud region, sensing altitudes of 45–50 km. In the polar region, thermal emission at 3.8 and 5.1 μm can also provide contrasts corresponding to the cloud top (∼65 km). Such observations were made from flyby and orbital missions, from Mariner 10 (Limaye & Suomi 1981) to the most recent Venus Express (e.g., Sanchez-Lavega et al. 2008, Khatuntsev et al. 2013) and Akatsuki (Nakamura et al. 2016) missions. A similar technique is also possible from recent ground-based observations (Sanchez-Lavega et al. 2017). Based on Pioneer Venus orbiter ultraviolet images, these cloud structures allowed observations of planetary-scale wave features at the cloud top (Del Genio & Rossow 1990). In addition to the 4.7-day equatorial zonal wind velocity, the so-called Y feature rotates with a 4-day period.

Contrasts can also be seen on the night side in emissions from O_2 (1.27 μm) and NO (190–300 nm) nightglow. Tracking these contrasts gives access to wind speeds at higher altitudes, around 95 km for O_2 and 110 km for NO (Drossart & Montmessin 2015). However, the hypothesis that these contrasts are relevant to track the background wind may be questionable.

The motion of the entry probes from the Venera 4, 7–10, 12, and 13 missions (Kerzhanovich & Marov 1983, Avduevskii et al. 1983) and from the Pioneer Venus mission (**Figure 1*a***; Counselman et al. 1980) were tracked to deduce vertical wind profiles at the entry sites. The Vega 1 and 2 missions provided both (*a*) a lander, and hence a vertical wind profile (Moroz & Zasova 1997), and (*b*) balloons that floated in the cloud layer, around 53 km altitude, providing horizontal and vertical wind velocities along the trajectories (Blamont et al. 1986, Linkin et al. 1986).

Based on the temperature fields retrieved from the Pioneer Venus (Seiff et al. 1980, Taylor et al. 1980), Venera 15 (Zasova et al. 2007), and Venus Express (e.g., Tellmann et al. 2009, Grassi et al. 2010) missions, the cyclostrophic thermal wind equation (Equation 1) was used to obtain thermal wind fields (e.g., Limaye 1985, Zasova et al. 2007, Piccialli et al. 2008, Mendonça et al. 2012). The latitudinal profile of the zonal wind at cloud top (around 70 km altitude) was also obtained using ground-based Doppler-shift measurements of reflected solar Fraunhofer lines (Widemann et al. 2008; Machado et al. 2012, 2017). This technique allows a direct measurement of the horizontal wind velocity and can help validate wind fields obtained from cloud tracking.

The zonal wind field is characterized by positive (i.e., same direction as the rotating planet below) values all over the planet for altitudes above roughly 10 km. Below that, the zonal wind velocity u is small (on the order of a few meters per second according to Pioneer Venus probes), and then it increases almost linearly with altitude to peak near the cloud top at velocities around 100–110 m/s. The latitudinal distribution is fairly constant for latitudes below 50°, then drops linearly with latitude toward zero near the poles. In the polar areas, the vertical shear appears to be weak in the cloud region. In some cloud-tracking data sets, the presence of a midlatitude jet near the cloud top is observed. This is also the case in the cyclostrophic zonal wind fields obtained from temperature fields. Some dependencies with local time (Del Genio & Rossow 1990) and with topography (Bertaux et al. 2016) have been observed, but they remain under active investigation.

2.3. Superrotation on Titan

Titan is also covered with a thick haze layer in the stratosphere (up to ∼300 km altitude), but there are almost no contrasting features that allow wind measurements at any wavelength. Cloud activity has been observed in the troposphere at wavelengths where the haze provides windows, but their variability makes it difficult to measure the wind speed with confidence. Before the Cassini/Huygens mission to the Saturnian system, very little data had been obtained on the

zonal wind field. Sparse cyclostrophic thermal wind values were obtained from Voyager Infrared Interferometer Spectrometer and Radiometer (IRIS) temperature retrievals (Flasar et al. 1981, Hanel et al. 1981), indicating large zonal wind velocities in the stratosphere. Stellar occultations observed from Earth-based telescopes provided additional information (Hubbard et al. 1993), showing high-latitude jets in the winter stratosphere at high latitudes, though the direction of the zonal wind could not be obtained this way.

This ambiguity was removed only with the use of Earth-based Doppler-shift measurements obtained from Earth-based telescopes when observing molecular constituent emission lines, such as infrared heterodyne spectroscopy on Titan's ethane emission lines near 12 μm (Kostiuk et al. 2001). The differential Doppler shift between eastern and western limbs confirmed the prograde direction of the zonal wind, with superrotation on the order of 200 m/s at around 1 hPa pressure (220 km), values supported by further observations (e.g., Kostiuk et al. 2010). This technique was also used on the visible spectrum (Luz et al. 2005) and with millimeter interferometry (Moreno et al. 2005).

The only in situ measurement of the zonal wind velocity has been the vertical profile obtained near the equator through the analysis of the Doppler Wind Experiment onboard the Huygens probe (**Figure 1*b***; Bird et al. 2005). Even though the experiment did not work as planned, the probe's motion could be tracked from Earth and the zonal wind profile retrieved. It shows a prograde velocity increasing with height from the surface to more than 100 m/s at 145 km, except for a peculiar minimum of zonal wind in the lower stratosphere, near 70–80 km altitude.

The most extensive data set for zonal winds on Titan is now obtained through cyclostrophic thermal winds based on Cassini Composite Infrared Spectrometer (CIRS) temperature fields. This data set captures the seasonal evolution of the superrotation from northern winter through northern spring equinox and into northern summer (Achterberg et al. 2008, 2011). The stratospheric zonal wind velocity peaks in the winter hemisphere at around 0.1 hPa (roughly 300 km), with maximum winds up to almost 200 m/s. In the summer hemisphere, the wind velocity decreases toward the pole from around 100 m/s near the equator. Between 2005 and 2009 (equinox), the maximum of the jet appeared to move slightly upward into the mesosphere, accompanied by a global increase in the summer hemisphere. These seasonal changes were monitored until the next solstice and the end of the mission, in fall 2017.

3. GENERAL CIRCULATION MODELS

To consolidate our understanding of the superrotation phenomenon, the use of atmospheric models is crucial. Though this has been a long and difficult progression, current atmospheric models are now able to reproduce the superrotation on Venus and Titan, and also to study this phenomenon, in a more idealized way, for other types of atmospheres.

3.1. Constituent Elements of a General Circulation Model

To simulate the climate of an atmospheric system, powerful tools have been developed, with capabilities improving as computer power has increased. In order to characterize the temperature and fluid velocity fields in the atmosphere, these General Circulation Models (GCMs) integrate in time a discretized set of nonlinear differential equations written in a spherical, rotating frame: the Navier-Stokes momentum equations, an equation for the conservation of energy, and an equation for the conservation of mass, together with the equation of state of the fluid. These equations are approximated and solved in the dynamical core. In addition, the system is forced by radiative transfer processes and other physical processes that need to be parameterized (surface exchanges

of energy and momentum, turbulence, convection). All these processes constitute the "physics" part of the GCM.

3.1.1. Dynamical cores. The design of the best form and approximations needed to solve the momentum, mass, and energy equations is a complex task. The main problems have been reviewed by Dowling (2013) for the Earth case and discussed by Forget & Lebonnois (2013) in a more general approach for the terrestrial planets. Once the equation set is defined, the discretization technique and grid will determine many of the properties of the dynamical core, the most important of all being its conservation properties for mass and energy. Finite-difference longitude-latitude grids have long been in competition with spectral cores that use truncated series of spherical harmonics. The most modern GCMs, however, tend to use horizontal grids with a quasi-uniform resolution over all of the grid, allowing massively parallel computing while avoiding polar singularity problems (Staniforth & Thuburn 2012, Dowling 2013). The vertical coordinate is another crucial choice: Altitude above reference geopotential, pressure, or mass each has its own advantages and problems, depending on how the equations are written (Holton 2004). Most of the time, hydrostatic equilibrium and a shallow atmosphere (compared to the solid radius of the planetary body) are significant approximations, leading to limitations that the modelers need to be aware of. As an example, the shallow-atmosphere approximation is poor when dealing with Titan's atmosphere, which extends to several hundreds of kilometers, compared with Titan's radius of only 2,575 km.

3.1.2. Radiative transfer. Computing the radiative transfer in the atmosphere has to be done in a fast yet precise enough way. Solar incident light is considered separately from the infrared thermal emission of the atmosphere. A simplified approach consists in relaxing the temperature structure toward a prescribed profile, with a time constant characteristic of the radiative processes. Although this approach does not allow a self-consistent computation of the temperature field, it has been used in many GCMs of the Venusian atmosphere, as radiative transfer appears to be complex in the case of Venus due to the high opacities of the dense CO_2 atmosphere and thick cloud layers (Eymet et al. 2009, Mendonça et al. 2015).

To deal with the spectral dimension, more and more planetary climate models use the correlated *k* distribution technique, which limits the number of variables, allowing description of the full line-by-line gas-phase absorption spectra in an efficient way (see, e.g., Eymet et al. 2009 and Mendonça et al. 2015 for various applications).

3.1.3. Additional parameterizations of physical processes. One of the essential physical processes to be taken into account is related to the interaction between surface and atmosphere, i.e., the computation of the boundary-layer conditions and resulting heat and momentum exchanges. These processes occur at scales much smaller than the typical size of grid cells and are dependent on tuned parameters. A boundary-layer scheme often used as a simple approach comes from Mellor & Yamada (1982).

The more physical processes included, the more GCMs become truly global models that incorporate the many phenomena that can affect the atmospheric system. These additional processes include, in particular, photochemistry to compute the atmospheric composition and microphysics to describe clouds or hazes. These components allow a GCM to include all couplings between dynamics, opacity sources, and radiative transfer. This is especially important for fully understanding the complex interactions in the climate systems of Titan and Venus, since both include thick, planet-covering layers of particles coupled to chemical cycles: hydrocarbon photochemistry producing dense stratospheric haze for Titan, and a sulfur cycle and dense sulfuric acid clouds for Venus.

3.2. Lessons from the Circulations of Venus and Titan

The development of GCMs has been strongly stimulated by space exploration: first of Venus in the late 1970s and early 1980s, then of Titan in the Cassini-Huygens era, and most recently of Venus again with the Venus Express mission. Reproducing the observed superrotation was not easy, and many questions were raised with the first GCMs of Venus's atmosphere (Young & Pollack 1977, Mayr & Harris 1983, Rossow 1983). After the first successful modeling of Titan's superrotation (Del Genio et al. 1993, Hourdin et al. 1995), a series of Venus GCM developments led to relatively successful GCMs after 2010, both for Venus (Lebonnois et al. 2010, Sugimoto et al. 2014a, Mendonça & Read 2016) and for Titan (Newman et al. 2011, Lebonnois et al. 2012a, Lora et al. 2015). Reviews of the evolution of GCMs are available from Lewis et al. (2013) and Sanchez-Lavega et al. (2017) for Venus and from Lebonnois et al. (2014) for Titan.

The source of the problems that affected the early GCM studies is not completely clear. Due to the crucial role of wave activity (as discussed below in Section 4), inadequate horizontal and/or vertical resolution may have underlain at least some of these problems. Angular momentum nonconservation is another candidate, although excessive vertical mixing of angular momentum associated with convective adjustment parameterizations, activated through incorrectly computed atmospheric static stability, may too have contributed (e.g., Del Genio et al. 1993). When such vertical mixing parameterizations are applied to momentum, angular momentum is transferred downgradient, which can overwhelm the tendencies of meridional overturning and wave driving to transfer angular momentum into upper levels (e.g., Read 1986). Superrotation ultimately results from the accumulation of angular momentum in an atmosphere, and it appears to be maintained through a subtle balance between large angular momentum transport terms. Tiny variations in the computation of the different terms in the balance may therefore result in a different distribution of zonal wind (Lebonnois et al. 2012b). An interesting illustration of the impact of small errors in the dynamical core on a strongly superrotating atmosphere was recently published by Lebonnois et al. (2013). Based on an exercise similar to the Held and Suarez benchmark used in Earth atmosphere modeling (Held & Suarez 1994), a large dispersion in the modeled zonal wind fields was obtained. Despite reproducing a similar qualitative shape of the zonal wind distributions, the amplitude of the superrotation and the position of the jets were very different among the GCM results. This strongly suggests that it is important to study and compare the behavior of several different GCMs before robust conclusions may be drawn on the controlling processes of a given superrotating atmosphere.

Titan's atmospheric simulations clearly confirm that the Gierasch-Rossow-Williams scenario (see Section 4.1) is effectively controlling Titan's atmospheric circulation. The crucial role of planetary-scale waves is demonstrated in the most recent successful GCMs (Newman et al. 2011, Lebonnois et al. 2012a, Lora et al. 2015): Barotropic activity in the stratosphere episodically transports angular momentum against the transport due to the mean meridional circulation, allowing equatorial superrotation to be maintained. An example of the modeled distribution of zonal winds is given in **Figure 4**. Titan's seasonal variations induce some complications in the details of the processes. There is also a potential problem related to the thickness of the atmosphere, which is not taken into account in the standard GCM cores.

A significant difference between the atmospheric circulations of Titan and Venus concerns thermal tides. On Titan, the long radiative adjustment timescales prevent diurnal tides from affecting the circulation, whereas on Venus, they play a major role in the equatorial vertical transport of angular momentum (Newman & Leovy 1992, Takagi & Matsuda 2007, Lebonnois et al. 2010). Venus GCMs have also illustrated the limitations of some modeling approaches. Where simple radiative forcings induce a mean meridional circulation with only one Hadley-type

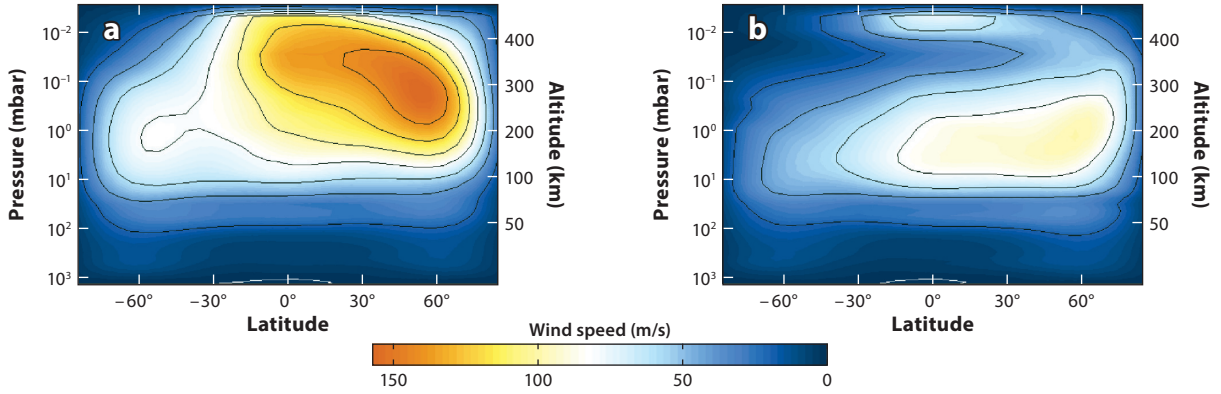

Figure 4

Titan modeled zonal-mean zonal winds for (*a*) northern midfall and (*b*) midwinter, modified from Lora et al. (2015) with permission from Elsevier.

cell centered in the deep atmosphere, ranging from the surface to the upper atmosphere, more recent GCMs with full radiative transfer (Lebonnois et al. 2010, 2016; Mendonça & Read 2016)—or simplified forcing with an improved prescription of the heating and cooling rates (Sugimoto et al. 2014a,b; Ando et al. 2016)—feature simulations with a strong Hadley-type cell in the cloud region (roughly 48–70 km altitude), another Hadley-type cell below the clouds, and a third one above the clouds (**Figure 5**).

The current GCMs for Venus and Titan now appear to be powerful (but sensitive) tools to explore the wave activity and the momentum balance in the circulation, and to help decipher the details of the mechanisms generating and maintaining the superrotation.

3.3. Exploring the Parameter Space

The transition to superrotating atmospheres was also studied using idealized Earth-like GCMs, varying some of the planetary parameters, such as the radius of the planet, to explore the regions of the parameter space where superrotation can arise. Mitchell & Vallis (2010) showed how an Earth-like atmosphere may transition from a weakly superrotating, Earth-like circulation to strong superrotation with increasing thermal Rossby number, the ratio of a characteristic horizontal (geostrophic) thermal wind speed U to the equatorial surface velocity $Ro_T = U/(2\Omega a)$. In their study, reducing the planet's radius to obtain thermal Rossby numbers much larger than 1 (such as for Venus and Titan) induced modifications in the dominant wave activity, with the development of a global disturbance of zonal wave number 1 that led to a convergence of angular momentum at the equator.

Dias Pinto & Mitchell (2014), however, showed that reducing only the rotation rate, even though it also reduces the thermal Rossby number, does not necessarily generate strong superrotation. They studied the influence of other nondimensional parameters, in particular a thermal damping number (the product of the thermal damping timescale and the planetary rotation rate). This number governs the thermal inertia of the atmosphere. In their simulations, when the rotation rate was reduced, superrotation developed only if the thermal damping number (which also depends on Ω) was maintained to high values. Otherwise, a very strong meridional circulation developed and inhibited the formation of the large-scale disturbances that are responsible for the production of equatorial superrotation.

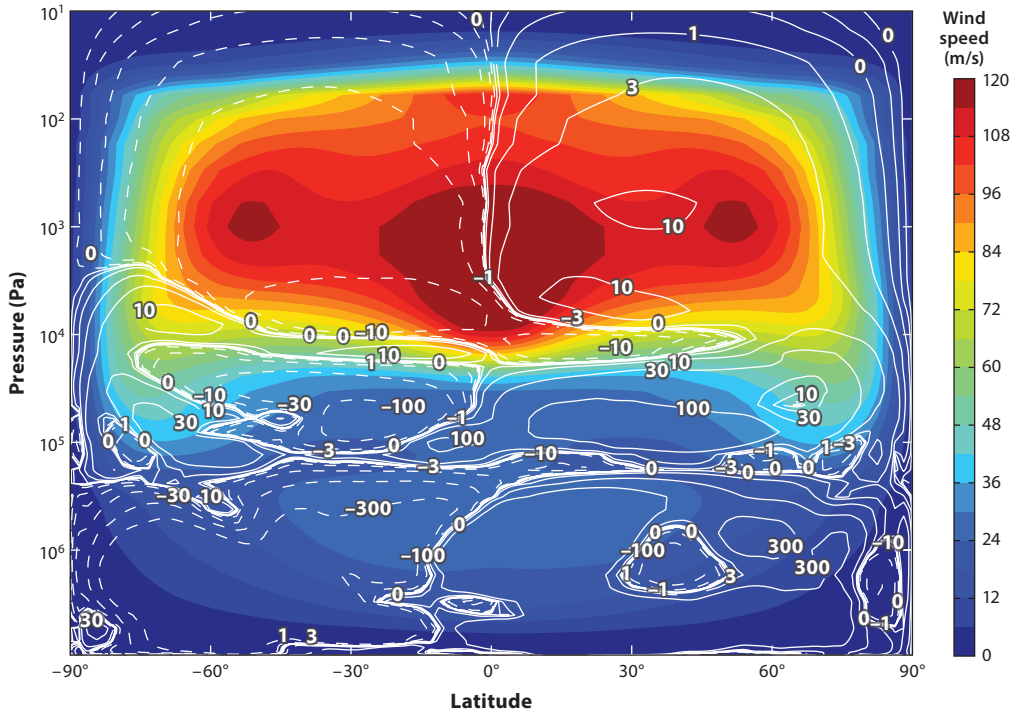

Figure 5

Venus modeled zonal-mean zonal winds, modified from Lebonnois et al. (2016) with permission from Elsevier. White contours show the averaged stream function (i.e., the mean meridional circulation) in units of 10^9 kilograms per second, solid contours indicate clockwise rotation, and dashed contours indicate counterclockwise rotation.

4. MECHANISMS FOR SUPERROTATION

4.1. The Gierasch-Rossow-Williams Scenario

The notion that the Hadley meridional circulation on Venus plays a major role in generating its superrotation in association with nonaxisymmetric eddies was originally suggested by Gierasch (1975), who devised a reasonably complete scenario for the production and maintenance of superrotation. This approach included a simple diffusive parameterization of the role of eddies in transporting angular momentum so as not to violate Hide's theorems. However, it was necessary to make certain assumptions about the way eddies mix momentum, vorticity, and heat in order not to neutralize thermal gradients or mix angular momentum in the vertical too effectively. Gierasch (1975) placed emphasis on the effects of eddies primarily as generic horizontal mixing agents of vorticity, which enables eddy diffusion to transport angular momentum upgradient in a similar manner to horizontal molecular viscosity (Plumb 1977, Read 1986). This emphasis on the role of eddies as horizontal vorticity mixers was taken up subsequently by Rossow & Williams (1979), who investigated the possible role of large-scale, barotropically unstable eddies under Venus-like conditions and also demonstrated numerical solutions of superrotating flows in a shallow-water model. These combined insights have led to an important paradigm in our understanding of superrotation and the formulation of conceptual models, now known as the Gierasch-Rossow-Williams (GRW) scenario.

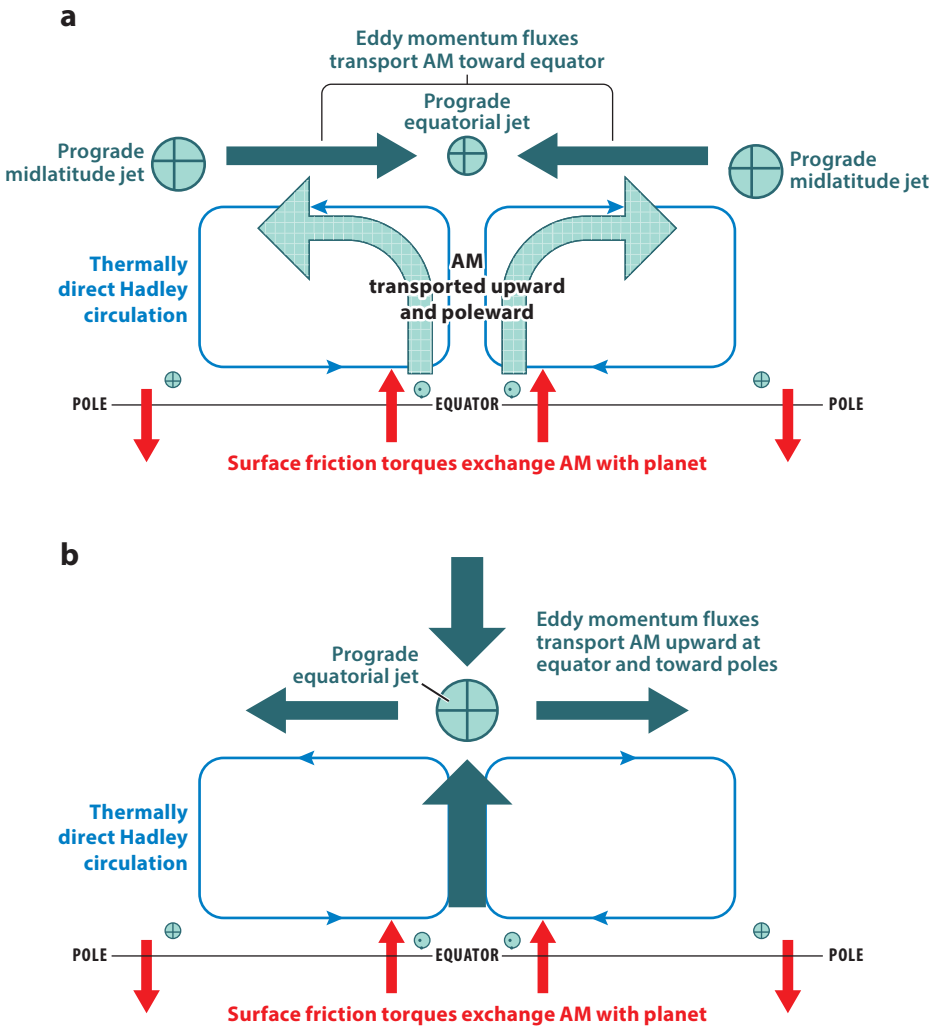

Figure 6

Schematic diagram illustrating the main features of (*a*) the classical Gierasch-Rossow-Williams scenario and (*b*) a nonclassical alternative scenario for atmospheric superrotation, in which upgradient fluxes of angular momentum (AM) occur in the vertical. Modified from Read (2013) with permission from Springer.

4.1.1. The classical Gierasch-Rossow-Williams scenario. The classical form of this scenario, as envisaged by Gierasch (1975), can be understood with reference to the schematic diagram in **Figure 6*a***, which illustrates the main transports and circulation processes.

Heating over the equator and cooling in polar regions respectively leads to rising and sinking motion as the Hadley overturning circulation is initiated from rest. Continuity of mass requires air near the surface to move toward the equator, roughly conserving its angular momentum as it moves along the surface. Hence, westward relative zonal flow is induced at low latitudes and is then acted upon by surface friction. Frictional drag weakens the westward near-surface flow, thereby increasing its absolute specific angular momentum and injecting positive m into the flow

(**Figure 6*a***). The newly injected m at the surface is thus effectively transported upward and poleward by the angular momentum–conserving poleward flow at upper levels (**Figure 6*a***).

Gierasch (1975) and Rossow & Williams (1979) supposed that the strong equator-pole shear in the upper-level flow leads to the generation of eddies, most likely from the action of an instability. These eddies are assumed to act to mix the flow toward a state of uniform vorticity. Here, there is an analogy with the effects of Newtonian viscosity, which acts to mix toward a state of solid body rotation and uniform angular velocity, since a flow with uniform angular velocity will also have a uniform vorticity with latitude. Thus, the development of such eddies will lead to a flux of angular momentum toward the equator, thereby setting the seed for the formation of a local maximum in m over the equator itself (**Figure 6*a***). As the flow equilibrates, eastward flow from the midlatitude jets extends toward the ground, allowing friction to remove angular momentum from the atmosphere and thereby providing a region of negative torque to balance the positive torque acting near the equator on the equatorward low-level flow. By this point, the upper-level flow has evolved toward a state of almost uniform absolute vorticity (and angular velocity) with an angular velocity that approaches that of the midlatitude jets. Such a flow will now have a strong positive maximum of m over the equator, and a superrotating state will have been attained.

The strength of the superrotation so attained is evidently dependent on a number of factors, but essentially, it requires the upper levels to become strongly isolated from the lower atmosphere so that the accumulation of angular momentum at upper midlatitudes does not leak away too rapidly. This requires stable static stability and requires the eddies to transport angular momentum preferentially in the horizontal direction. Gierasch (1975) estimates the strength of superrotation to depend on the dimensionless parameter

$$S_G = (D\tau_v/H\tau_d) = \frac{WD}{\nu_v}, \qquad 6.$$

where D/H is the depth of the atmospheric circulation normalized by the pressure scale height, H; τ_v is the timescale associated with vertical diffusion of momentum; τ_d is the dynamical overturning timescale of the Hadley circulation with vertical velocity scale W; and ν_v is the vertical eddy viscosity. When S_G is large, strong superrotation will be observed; if it is small, for example, because the circulation is shallow or the vertical eddy mixing is very efficient, then superrotation will be comparatively weak.

Gierasch (1975) did not discuss in detail the nature of the main eddies in this scenario; Rossow & Williams (1979) proposed that large-scale waves and eddies formed from barotropic instability would transfer angular momentum in the poleward direction, but this is by no means the only possible configuration. Indeed, one of the key issues in understanding Venus's atmospheric circulation is the nature and role of various eddy processes in transporting angular momentum and contributing to sustaining superrotation.

4.1.2. A nonclassical Gierasch-Rossow-Williams scenario. An alternative scenario is illustrated in **Figure 6*b***. In this case, a thermally direct Hadley circulation acts as before to extract angular momentum from the solid planet in the tropics during spin-up, and to transport m upward and poleward to form midlatitude jets. Unlike in the classical GRW scenario, however, the eddies are now assumed to transport m predominantly upgradient in the vertical direction instead of in the horizontal. Such a configuration can be equally valid in the context of Hide's theorems (cf. Section 1.1), provided any horizontal momentum fluxes are predominantly poleward instead of equatorward.

Eddies acting in this way are likely to have a quite different origin from the predominantly barotropic eddies invoked in the classical GRW mechanism, but there are a number of plausible candidates. These and the likely waves and eddies contributing to the GRW mechanism are considered in the next section.

4.2. Eddy–Zonal Flow Interactions

The simplest approach to considering the effect of eddies in transporting angular momentum and influencing the zonal mean circulation in the classical GRW scenario (Gierasch 1975, Rossow & Williams 1979) was to assume that they act as a simple momentum-mixing agent in the horizontal, analogous to an eddy viscosity. Such an assumption leads to a tendency for eddies to mix toward a state of uniform angular velocity, which may also correspond to a state of minimum kinetic energy, given a prescribed zonal momentum (Rossby 1947). Gierasch (1975) also found it necessary, however, to neglect angular momentum mixing in the vertical, and to neglect thermal "diffusion" by eddies altogether; otherwise, efficient horizontal mixing of heat would eliminate horizontal thermal gradients too efficiently to reach a realistic equilibrium (e.g., Kálnay de Rivas 1975).

This approach to eddy–zonal flow interactions as a quasi-viscous process assumes that eddies are homogeneous, isotropic, and effectively passive entities that behave like colliding particles, by analogy with the classical kinetic theory of gases (e.g., Chapman & Cowling 1970). But this is quite an unrealistic characterization of eddies typically found in a planetary atmosphere, especially on large scales, where the effects of planetary rotation and spherical curvature cause eddies to acquire a more wavelike character that may be highly anisotropic and inhomogeneous.

More generally, nonlinear wave–zonal flow interactions behave quite differently (Held 1975, Andrews & McIntyre 1976, Edmon et al. 1980), tending to accelerate zonal flows in the opposite direction to their phase speed in regions where they are being generated and in the same sense as their phase speed where they are dissipated. For rapidly rotating planets, the dominant type of waves on large scales are Rossby-Haurwitz waves, which tend to propagate westward relative to their background flow. Thus, Rossby wave sources on the equator would tend to accelerate local superrotation close to the equator and drive retrograde flow at poleward latitudes where they dissipate. A mid- or high-latitude source of Rossby waves, however, would tend to accelerate prograde zonal flow at high latitudes and lead to equatorial subrotation in association with poleward angular momentum fluxes if Rossby wave action is dissipated in the tropics. For Earth-like, rapidly rotating planets, therefore, Laraia & Schneider (2015) suggested that the tendency of an atmosphere to super- or subrotate at the equator depends rather critically upon the relative strengths of the sources of Rossby wave activity at the equator and at higher latitudes.

Sources of Rossby wave activity in the tropics can include localized heat sources, which can lead to strongly divergent flows that launch Rossby waves poleward (e.g., Suarez & Duffy 1992, Saravanan 1993, Kraucunas & Hartmann 2005, Arnold et al. 2012). This is essentially the mechanism that underlies the generation of superrotating jets in model simulations of tidally locked exoplanets, with a strong region of local heating around the substellar point on the equator (e.g., Joshi et al. 1997, Merlis & Schneider 2010, Pierrehumbert 2011). The heated region leads to upper-level horizontal divergence (Sobel et al. 2001), which, in turn, can generate large-scale rotational flow and Rossby waves, either through vortex stretching or vorticity advection (Sardeshmukh & Hoskins 1988). Alternatively, other forms of local instability might lead to the generation of Rossby wave activity near the equator. Wang & Mitchell (2014) and Dias Pinto & Mitchell (2014), for example, recently suggested that a Rossby-Kelvin instability centered on the equator may produce a convergence of angular momentum and lead to the formation of superrotation.

On Earth, however, these processes must compete with the generation of Rossby wave activity by intense baroclinic instabilities at midlatitudes. Rossby waves produced by this process may dissipate in the tropics, leading to a strong tendency for subrotation. The latter process evidently tends to win most of the time in the troposphere, such that horizontal eddy momentum fluxes are predominantly poleward, although equatorial superrotation remains a possibility were there to be an event that enhanced Rossby wave generation in the tropics.

This property of Rossby waves poses some difficulties for the basic Gierasch (1975) picture of superrotation, since this scenario relies on eddies being generated by an instability at high latitudes and mixing angular momentum equatorward from the prograde zonal jets at the poleward edges of the Hadley cells. For slowly rotating planets, however, Rossby waves are not the only wave modes that may be significant in transporting heat and momentum across the planet. In the absence of strongly sheared zonal flows, the full spectrum of eigenmodes of Laplace's tidal equations (also known as the shallow-water equations) includes several families of waves, characterized by integer indices ν and ν' (e.g., Longuet-Higgins 1968, Andrews et al. 1987) and capable of propagating with phase speeds that are either westward or eastward. Eastward-propagating modes include high-frequency inertia-gravity waves ($\nu \geq 0$) and the equatorially trapped Kelvin mode ($\nu' = 0$). Westward-propagating modes again include high-frequency inertia-gravity waves ($\nu \geq 1$), similar to their eastward counterparts; low-frequency planetary Rossby waves ($\nu' \geq 1$); and the intermediate mixed planetary gravity mode ($\nu = 0$). Such modes are also capable of propagating vertically in a stratified atmosphere, so they will also carry angular momentum upward or downward.

Directly forced waves provide an alternative source of wave activity with phase speeds dictated by the forcing itself. A particularly important category in the context of Venus (as mentioned in Section 3) includes the diurnal and semidiurnal tides, induced by the day-night contrast in radiative heating and cooling. These sun-synchronous tides propagate in phase with the subsolar longitude, so they move westward relative to the underlying planet. Thus, diurnal tides can be a driver of superrotation in regions where they are excited by radiative forcing, which are typically at low latitudes, and of subrotation where they are dissipated (e.g., Fels & Lindzen 1974, Pechmann & Ingersoll 1984, Baker & Leovy 1987).

There is, therefore, no shortage of possible wave processes that could contribute to initiating and maintaining equatorial and/or global atmospheric superrotation. But precisely which processes are dominant in a given situation may be highly dependent on the circumstances of each planet.

5. SUPERROTATION ON TITAN AND VENUS?

Discussion so far has dealt with the general issues of how to quantify atmospheric superrotation, where it occurs within the Solar System and beyond, and general dynamical mechanisms that can lead to the emergence of sustained superrotation. But when it comes to specific planets, the devil is in the quantitative detail. For Titan and Venus, which exhibit the most extreme forms of superrotation, direct observations are able to provide some quantitative confirmation of the occurrence of strong superrotation in their atmospheres, but despite the wealth of data from missions such as Pioneer Venus and Venus Express, they are not sufficient to confirm conclusively precisely which processes dominate the generation and maintenance of the observed superrotation. The elucidation of precisely how the angular momentum budget for each atmosphere is sustained is therefore largely dependent upon the analysis of numerical model simulations. As discussed in Section 3, however, this introduces a number of uncertainties associated with how such models are formulated, even when the simulation is able to achieve realistic levels of superrotation in the places where it is observed. With this proviso, therefore, we go on to review what appears to be the most likely scenario for superrotation on Titan and on Venus.

5.1. Which Scenario for Titan?

As for Venus, achieving realistic peak wind speeds and levels of superrotation in Titan GCMs has proved challenging for generations of such models, particularly when the parameterizations of radiative transfer and subgrid-scale processes have been designed to be as quantitatively realistic as possible. As discussed above, three recent models (Newman et al. 2011, Lebonnois et al. 2012a, Lora et al. 2015) appear to achieve quantitatively realistic simulated circulations with observationally reasonable levels of superrotation.

All three models spin up to a circulation dominated by planetary-scale Hadley-type meridional overturning circulations, suggestive of at least one ingredient of the GRW scenario. These are not simple unicellular patterns in each hemisphere, however, with some evidence for counterrotating cells at high latitudes and some complex structure in the vertical. But the overall, annually averaged effect in all three models is to transport angular momentum upward at low latitudes into the stratosphere and then poleward. This leads to an angular momentum deficit close to the surface during the spin-up of the circulation, which, in turn, allows surface processes to extract angular momentum from the solid planet. At equilibrium, however, the circulation is modified at high latitudes, enabling the overall torque between atmosphere and solid planet to reduce to very small values, though not necessarily to zero because of imperfections in the way different model formulations conserve and transport angular momentum or parameterize subgrid-scale mixing (e.g., see Hourdin et al. 1995, Lora et al. 2015).

A further complication on Titan is the variation in time associated with the seasonal cycle, which shifts the meridional overturning circulation back and forth in latitude. The modeled mean zonal flow also responds to seasonal variations, which are then reflected in the overall global superrotation that therefore fluctuates throughout the Titanian year by around $\pm 4 \times 10^{24}$ (kg·m^2)/s (i.e., around ±1% of the mean value). Seasonal variations also affect the eddy component of the circulation, although the net horizontal transport of angular momentum in Titan's stratosphere by the resolved eddies in all of the main models is predominantly equatorward (Del Genio et al. 1993, Hourdin et al. 1995, Newman et al. 2011, Lebonnois et al. 2012a, Lora et al. 2015). The origin of these eddies in all these models appears to be from a combination of equatorially focused inertial instabilities and barotropic instabilities located on the equatorward flank of the winter high-latitude zonal jet. The precise partitioning of the transport between these respective processes is quite uncertain, however, since (*a*) barotropic instability depends closely upon the precise structure of the winter zonal jet and (*b*) the manifestation and development of inertial instabilities depend rather critically on model resolution and numerical formulation. In the troposphere (around altitudes of 0–40 km), however, some models show poleward transport of angular momentum at high latitudes (poleward of the midlatitude jet), which Lebonnois et al. (2012a) suggested may reflect a predominantly baroclinic instability. A similar form of low-frequency wave was also found in more idealized simulations of slowly rotating atmospheric circulations by Mitchell & Vallis (2010) and in a troposphere-only Titan GCM by Mitchell et al. (2011), though there are few observations to confirm this.

The radiative adjustment timescale on Titan is generally too long for diurnal variations to be of much significance in the troposphere or midstratosphere (Hourdin et al. 1995, Lebonnois et al. 2012a), even though some diurnal effects on clouds and boundary-layer convection are evident (Charnay & Lebonnois 2012, Burgalat et al. 2014). This has been largely confirmed in model simulations that compare circulations with and without a diurnal cycle represented (e.g., Lebonnois et al. 2012a). The results show little impact of the diurnal cycle on atmospheric angular momentum and transport, indicating that diurnal tides play little or no role on Titan in its superrotation.

5.2. Which Scenario for Venus?

A similar overall scenario is also relevant to Venus, although the quantitative balances may be somewhat different. The pattern of zonal winds obtained in the most comprehensive physical models (e.g., Lebonnois et al. 2010, Sugimoto et al. 2014a, Mendonça & Read 2016) seems quite realistic at the levels of the main cloud decks and above (with variable evidence of high-latitude zonal jets superposed on a rapid solid body rotation with rotation period ∼4 Earth days) but arguably less so at deeper levels. As a result, the mass-weighted global superrotation indices obtained in the modeled circulations tend to be quite a lot smaller than the observations would suggest. Nevertheless, the simulations seem to be sufficiently realistic around the cloud levels to draw some reasonable conclusions about the planet itself, though some caution must be exercised in the interpretation of the deeper levels.

Observations certainly point to the existence of large-scale meridional overturning circulations between the tropics and high latitudes, which would tend to transfer angular momentum upward and poleward. Quantitatively realistic models, however, suggest that this Hadley-like circulation pattern on Venus is most intense near the levels of the main cloud decks (e.g., Lebonnois et al. 2010, 2016; Mendonça & Read 2016), where much of the incoming solar energy is absorbed. At deeper levels, models suggest that the meridional overturning is much weaker and more complex in both space and time, with features suggestive of axisymmetric inertial instabilities close to the equator. Diagnostics of the angular momentum transport suggest that the mean meridional overturning circulation is one of the dominant terms in the angular momentum budget. In contrast to Titan, however, the obliquity of Venus is very small, so seasonal modulations are commensurately very weak (and not generally taken into account in GCMs).

The roles of nonaxisymmetric waves and other features also differ markedly from those on Titan. On a planetary scale, several models reproduce the formation of non-Sun-synchronous structures resembling the Y feature frequently seen in ultraviolet images of the planet. More detailed analyses suggest these to consist of a superposition of an equatorial Kelvin-like mode of zonal wavenumber 1, centered on the equator, and an equatorial Rossby-like mode that is symmetrical about the equator (Sugimoto et al. 2014b, Lebonnois et al. 2016). The Kelvin mode appears just above the main cloud deck at altitudes of 50–60 km, which is consistent with being forced by statically unstable convection within the underlying cloud deck. The role of this Kelvin mode was also put forward in a theoretical study of Venus waves (Peralta et al. 2015). The Rossby mode, on the other hand, may be associated with barotropically unstable regions at higher latitudes. The resultant large-scale wave pattern does appear to be consistent with a mean eddy transport of angular momentum toward the equator, as required in the classical GRW scenario, although the Kelvin wave component would likely result in some vertical transport of angular momentum upward from the cloud decks (where it is generated) to higher levels (where it dissipates). However, Sugimoto et al. (2014b) have suggested that at higher latitudes the zonal flow is baroclinically unstable, somewhat as on Titan, though the direction of angular momentum transfer by this process is somewhat unclear. But there is direct evidence of a complex wave pattern over both poles with zonal wavenumber 2 (a dipole) or 3, which evidently changes rapidly with time, indicative of an active instability (Yamamoto & Takahashi 2015, Ando et al. 2016).

In strong contrast with that on Titan, however, the diurnal cycle on Venus evidently plays a much stronger role, which some (Takagi & Matsuda 2007, Sugimoto et al. 2014a) have suggested may even be dominant in maintaining Venus's superrotation. Model studies that have compared the circulation simulated with and without a diurnal cycle (Lebonnois et al. 2010) suggest that the thermal tide has a strong impact on the strength of the zonal flow, with diurnally forced flows achieving

significantly stronger superrotation. Estimates of the radiative relaxation timescale in the Venus atmosphere (Pollack & Young 1975, Sugimoto et al. 2014a) indicate that this is comparable to, or shorter than, the Venus solar day at altitudes $\geq$50–60 km. A strong zonal wavenumber 2 pattern, stationary in a solar-fixed reference frame, is clearly visible in infrared measurements above the main cloud tops (Schofield & Taylor 1983), indicative of a semidiurnal thermal tide. At higher altitudes ($\gtrsim$70 km), this pattern dominates the structure of the atmosphere, driving a strong subsolar to antisolar circulation that dominates over the basic meridional overturning circulation that prevails at lower altitudes. The impact of this diurnally forced component of the circulation on angular momentum transport is to transfer m vertically downward above the main clouds (Pechmann & Ingersoll 1984), effectively accelerating the superrotation near the main cloud deck at the expense of the zonal motion higher up. The resulting balance therefore has some features in common with the nonclassical GRW scenario discussed in Section 4.1, although the complete picture is probably a complex mixture of the two.

6. OPEN ISSUES

The previous section summarizes the overall scenarios that reflect the dominant contributions to the angular momentum budget simulated by the best available numerical models of the atmospheric circulations of Venus and Titan. Such simulations have been validated as far as possible against available observations and measurements, and at least serve to demonstrate the ability of the scenarios to support patterns of local and global superrotation that approach the values found in nature. But there are a host of uncertainties that remain, despite the apparent success of these models.

The sensitivity of the simulated circulations of the atmospheres of slowly rotating planets to numerical formulations and resolution (Lebonnois et al. 2012b) is a significant concern that needs further investigation in the future. The development of such strong global superrotation in an atmosphere presents huge challenges to numerical schemes, which need to eliminate as much as possible any spurious sources or sinks of angular momentum that can distort the global or local budget. Such issues are made even more significant because of the sparseness of verifying measurements from both Venus and Titan, especially concerning the winds in their deep atmospheres.

Superrotation in the Venus atmosphere below the main cloud decks appears to be one aspect that challenges even the best GCMs, all of which seem to fail to reproduce adequately the slow decay with increasing depth of the zonal winds from the cloud levels toward the surface (e.g., Lebonnois et al. 2010, Mendonça & Read 2016). The reasons for this are still unclear, though it does point toward some missing physics in all of these models. Recent work (Lebonnois et al. 2016) suggests that increasing the spatial resolution of the model may reduce the disagreement with observations, although the simulated winds still differ by a factor of $\sim$2 from the observations, even with a spatial resolution of 96 $\times$ 96 points in latitude $\times$ longitude.

This improvement with resolution might suggest that small-scale internal gravity waves are playing an important role (although the spurious residuals in the numerical angular momentum budget may not be negligible). There is certainly plenty of observational evidence for the existence of such gravity waves in the Venus atmosphere, from entry probes and balloons (e.g., Counselman et al. 1980; Seiff et al. 1980; Young et al. 1987, 1994), radio-occultation measurements (e.g., Kliore & Patel 1980, Tellmann et al. 2009), and infrared images (Peralta et al. 2008). But these waves commonly occur on very small scales and are spatially very inhomogeneous and so have not yet been sufficiently well characterized for their effects to be parameterized in GCMs. Their origins are also quite unclear, although some are clearly linked with the underlying topography (Young et al. 1987, Tellmann et al. 2012, Fukuhara et al. 2017), while others may be linked to the

cloud-level convection or polar vortices. Similar kinds of internal gravity waves have also been found in Titan's stratosphere (e.g., Hinson & Tyler 1983, Friedson 1994, Sicardy et al. 1999), raising similar issues for the role of such waves in Titan GCMs.

The role of topography in generating and maintaining the levels of superrotation found on Venus and Titan is another question that models have yet to settle. The surface topography of Venus is well known from Pioneer Venus, Magellan, and Venera 15 radar mapping (e.g., Ford & Pettengill 1992) and has been incorporated into Venus GCMs. For Titan, topography was recently partially obtained from Cassini radar data and extrapolated at least on large scales (Lorenz et al. 2013), but it has not yet been taken into account in Titan GCMs. The presence of such topography would be expected to enhance the coupling of the atmosphere to the surface through the effects of mountain torques and mechanically induced turbulent mixing. Yet some model studies that have investigated the sensitivity of simulated Venus-like circulations to the presence or absence of realistic topography have suggested rather a small impact on the simulated superrotation (Herrnstein & Dowling 2007). Other models, however, suggest the opposite (e.g., Lebonnois et al. 2010), with topography having a substantial effect on the simulated circulation. This is clearly another area that needs further work to establish the role of topography more robustly.

A final question that remains somewhat open is why the local and global superrotation of the atmospheres of Titan and Venus is so much stronger than on other planets. Part of the answer lies within the Gierasch (1975) model itself, which predicts that $s \sim e^{S_G}$ (cf. Equation 6). This suggests that s (and also by implication S_m) $\gtrsim 1$ is strongly favored in circulations with strong and deep meridional overturning circulations and weak vertical mixing. This does, however, require the atmosphere to be in a weak horizontal temperature gradient regime, which restricts its applicability to tropical regions and also therefore favors slowly rotating systems for which the tropical Hadley circulation extends across much of the planet. Support for such a trend is apparent in some studies that use idealized Earth-like models to explore the parameter dependence of various atmospheric properties (e.g., Del Genio & Zhou 1996), for which slow rotators do tend to exhibit positive local and global superrotation regardless of the eddy processes that are represented. But this should be explored in more detail to elucidate the quantitative dependence more thoroughly. The role of the diurnal tide in the case of Venus, as well as the potential role of small-scale gravity waves and other processes, remains to be fully explored.

SUMMARY POINTS

1. Atmospheric superrotation is widespread (though not universal) among both terrestrial and gas giant planets, but the degree of superrotation varies greatly depending upon a number of parameters.
2. The so-called Gierasch-Rossow-Williams mechanism seems to capture the essence of how almost all slowly rotating planets develop a strong atmospheric superrotation, although planets differ markedly in the details of how eddies act to balance angular momentum transports produced by the dominant thermally direct meridional overturning circulation.
3. Strong superrotation is favored on slowly rotating planets with deep, stably stratified atmospheres that are optically thick and with circulations that are strongly radiatively driven well away from their underlying surface.

4. Titan and Venus represent extreme cases of very strong superrotation, such that their atmospheres rotate locally much faster than their underlying planets.
5. Despite the challenges involved, numerical models appear capable in principle of capturing the generation and maintenance of such strong superrotation, although the results are sensitive to the model formulation.

FUTURE ISSUES

1. More observations are urgently needed of the wind structure of the circulation of both Venus and Titan, especially at levels below the main cloud decks on Venus, and more generally of waves and eddies at all levels on Titan.
2. Further General Circulation Model studies are needed to explore the dependence of superrotation in simulated circulations on factors such as planetary rotation rate, vertical scales of motion, and model formulation and resolution.
3. The possible role of small-scale gravity waves in generating and maintaining superrotation should be investigated more thoroughly in future work.
4. The influence of surface topography on the angular momentum budget of slowly rotating planetary atmospheres should be studied further.

DISCLOSURE STATEMENT

The authors are not aware of any affiliations, memberships, funding, or financial holdings that might be perceived as affecting the objectivity of this review.

ACKNOWLEDGMENTS

We are grateful to the late Raymond Hide CBE FRS for his many insights on this problem. P.L.R. acknowledges support under UK Science and Technology Facilities Council grants ST/K00106X/1, ST/I001948/1, and ST/N00082X/1.

LITERATURE CITED

Achterberg RK, Conrath BJ, Gierasch PJ, Flasar FM, Nixon CA. 2008. Titan's middle-atmospheric temperatures and dynamics observed by the Cassini Composite Infrared Spectrometer. *Icarus* 194:263–77

Achterberg RK, Gierasch PJ, Conrath BJ, Flasar FM, Nixon CA. 2011. Temporal variations of Titan's middle atmospheric temperatures from 2004 to 2009 observed by Cassini/CIRS. *Icarus* 211:686–98

Ando H, Sugimoto N, Takagi M, Kashimura H, Imamura T, Matsuda Y. 2016. The puzzling Venusian polar atmospheric structure reproduced by a general circulation model. *Nat. Comm.* 7:10398

Andrews DG, Holton JR, Leovy CB. 1987. *Middle Atmosphere Dynamics*. Orlando, FL: Academic Press

Andrews DG, McIntyre ME. 1976. Planetary waves in horizontal and vertical shear: the generalized Eliassen-Palm relation and the mean zonal acceleration. *J. Atmos. Sci.* 33:2031–48

Arnold NP, Tziperman E, Farrell B. 2012. Abrupt transition to strong superrotation driven by equatorial wave resonance in an idealized GCM. *J. Atmos. Sci.* 69:626–40

Avduevskii VS, Marov MY, Kulikov YN, Shari VP, Gorbachevskiy AY, et al. 1983. Structure and parameters of the Venus atmosphere according to Venera Probe data. In *Venus*, ed. DM Hunten, L Colin, TM Donahue, VI Moroz, pp. 280–98. Tucson: Univ. Ariz. Press

Baker NL, Leovy CB. 1987. Zonal winds near Venus' cloud top level: a model study of the interaction between the zonal mean circulation and the semidiurnal tide. *Icarus* 69:202–20

Baldwin MP, Gray LJ, Dunkerton TJ, Hamilton K, Haynes PH, et al. 2001. The quasi-biennial oscillation. *Rev. Geophys.* 39:179–229

Barnes JR, Haberle RM, Wilson RJ, Lewis SR, Murphy JR, Read PL. 2017. The global circulation. In *The Atmosphere and Climate of Mars*, ed. RM Haberle, T Clancy, F Forget, MD Smith, RW Zurek, pp. 229–94. Cambridge, UK: Cambridge Univ. Press

Bertaux JL, Khatuntsev IV, Hauchecorne A, Markiewicz WJ, Marcq E, et al. 2016. Influence of Venus topography on the zonal wind and UV albedo at cloud top level: the role of stationary gravity waves. *J. Geophys. Res. Planets* 121:1087–101

Bird MK, Allison M, Asmar SW, Atkinson DH, Avruch IM, et al. 2005. The vertical profile of winds on Titan. *Nature* 438:800–2

Blamont JE, Young RE, Seiff A, Ragent B, Sagdeev R, et al. 1986. Implications of the VEGA Venus balloon results for Venus atmospheric dynamics. *Science* 231:1422–25

Burgalat J, Rannou P, Cours T, Rivière ED. 2014. Modeling cloud microphysics using a two-moments hybrid bulk/bin scheme for use in Titan's climate models: application to the annual and diurnal cycles. *Icarus* 231:310–22

Chapman S, Cowling TG. 1970. *The Mathematical Theory of Non-Uniform Gases*. Cambridge, UK: Cambridge Univ. Press. 3rd ed.

Charnay B, Lebonnois S. 2012. Two boundary layers in Titan's lower troposphere inferred from a climate model. *Nat. Geosci.* 5:106–9

Counselman CC III, Gourevitch SA, King RW, Loriot GB. 1980. Zonal and meridional circulation of the lower atmosphere of Venus determined by radio interferometry. *J. Geophys. Res.* 85:8026–30

Del Genio AD, Achterberg RK, Baines KH, Flasar FM, Read PL, et al. 2009. Saturn atmospheric structure and dynamics. In *Saturn from Cassini-Huygens*, ed. M Dougherty, L Esposito, S Krimigis, pp. 113–60. Dordrecht, Neth.: Springer

Del Genio AD, Rossow WB. 1990. Planetary-scale waves and the cyclic nature of cloud top dynamics on Venus. *J. Atmos. Sci.* 47:293–318

Del Genio AD, Zhou W. 1996. Simulations of superrotation on slowly rotating planets: sensitivity to rotation and initial conditions. *Icarus* 120:332–43

Del Genio AD, Zhou W, Eichler TP. 1993. Equatorial superrotation in a slowly rotating GCM: implications for Titan and Venus. *Icarus* 101:1–17

Dias Pinto JR, Mitchell JL. 2014. Atmospheric superrotation in an idealized GCM: parameter dependence of the eddy response. *Icarus* 238:93–109

Dowling TE. 2013. Earth general circulation models. In *Comparative Climatology of Terrestrial Planets*, ed. SJ Mackwell, AA Simon-Miller, JW Harder, MA Bullock, pp. 193–211. Tucson: Univ. Ariz. Press

Drossart P, Montmessin F. 2015. The legacy of Venus Express: nightlights from the first European planetary mission to Venus. *Astron. Astrophys. Rev.* 23:5

Edmon HJ Jr., Hoskins BJ, McIntyre ME. 1980. Eliassen-Palm cross sections for the troposphere. *J. Atmos. Sci.* 37:2600–16

Eymet V, Fournier R, Dufresne JL, Lebonnois S, Hourdin F, Bullock MA. 2009. Net-exchange parameterization of the thermal infrared radiative transfer in Venus' atmosphere. *J. Geophys. Res.* 114:E11008

Fels SB, Lindzen RS. 1974. The interaction of thermally excited gravity waves with mean flows. *Geophys. Fluid Dyn.* 6:149–91

Flasar FM. 1986. Global dynamics and thermal structure of Jupiter's atmosphere. *Icarus* 65:280–303

Flasar FM, Kunde VG, Achterberg RK, Conrath BJ, Simon-Miller AA, et al. 2004. An intense stratospheric jet on Jupiter. *Nature* 427:132–35

Flasar FM, Samuelson RE, Conrath BJ. 1981. Titan's atmosphere: temperature and dynamics. *Nature* 292:693–98

Ford PG, Pettengill GH. 1992. Venus topography and kilometer-scale slopes. *J. Geophys. Res.* 97:13103–14
Forget F, Bertrand T, Vangvichith M, Leconte J, Millour E, Lellouch E. 2017. A post-New Horizons global climate model of Pluto including the N_2, CH_4 and CO cycles. *Icarus* 287:54–71
Forget F, Lebonnois S. 2013. Global climate models of the terrestrial planets. In *Comparative Climatology of Terrestrial Planets*, ed. SJ Mackwell, AA Simon-Miller, JW Harder, MA Bullock, pp. 213–29. Tucson: Univ. Ariz. Press
Friedson AJ. 1994. Gravity waves in Titan's atmosphere. *Icarus* 109:40–57
Fukuhara T, Futaguchi M, Hashimoto GL, Horinouchi T, Imamura T, et al. 2017. Large stationary gravity wave in the atmosphere of Venus. *Nat. Geosci.* 10:85–88
Gierasch PJ. 1975. Meridional circulation and the maintenance of the Venus atmospheric rotation. *J. Atmos. Sci.* 32:1038–44
Glatzmaier GA, Roberts PH. 1996. Rotation and magnetism of Earth's inner core. *Science* 274:1887–91
Grassi D, Migliorini A, Montabone L, Lebonnois S, Cardesin-Moinelo A, et al. 2010. The thermal structure of Venusian night-time mesosphere as observed by VIRTIS-Venus Express. *J. Geophys. Res.* 115:E09007
Hammel HB, De Pater I, Gibbard SG, Lockwood GW, Rages K. 2005. Uranus in 2003: zonal winds, banded structure, and discrete features. *Icarus* 175:534–45
Hanel R, Conrath B, Flasar FM, Kunde V, Maguire W, et al. 1981. Infrared observations of the Saturnian system from Voyager 1. *Science* 212:192–200
Held IM. 1975. Momentum transport by quasi-geostrophic eddies. *J. Atmos. Sci.* 32:1494–97
Held IM, Hou AY. 1980. Nonlinear axially symmetric circulations in a nearly inviscid atmosphere. *J. Atmos. Sci.* 37:515–33
Held IM, Suarez MJ. 1994. A proposal for the intercomparison of the dynamical cores of atmospheric general circulation models. *Bull. Am. Meteorol. Soc.* 75:1825–30
Herrnstein A, Dowling TE. 2007. Effect of topography on the spin-up of a Venus atmospheric model. *J. Geophys. Res.* 112:E04S08
Hide R. 1969. Dynamics of the atmospheres of the major planets, with an appendix on the viscous boundary layer at the rigid bounding surface of an electrically-conducting rotating fluid in the presence of a magnetic field. *J. Atmos. Sci.* 26:841–53
Hinson DP, Tyler GL. 1983. Internal gravity waves in Titan's atmosphere observed by Voyager radio occultation. *Icarus* 54:337–52
Holton JR. 2004. *An Introduction to Dynamic Meteorology*. Amsterdam: Academic Press. 4th ed.
Hourdin F, Talagrand O, Sadourny R, Courtin R, Gautier D, McKay CP. 1995. Numerical simulation of the general circulation of the atmosphere of Titan. *Icarus* 117:358–74
Hubbard WB, Sicardy B, Miles R, Hollis AJ, Forrest RW, et al. 1993. The occultation of 28 Sgr by Titan. *Astron. Astrophys.* 269:541–63
Joshi M, Haberle R, Reynolds R. 1997. Simulations of the atmospheres of synchronously rotating terrestrial planets orbiting M dwarfs: conditions for atmospheric collapse and the implications for habitability. *Icarus* 129:450–65
Kálnay de Rivas E. 1975. Further numerical calculations of the circulation of the atmosphere of Venus. *J. Atmos. Sci.* 32:1017–24
Kerzhanovich VV, Marov MI. 1983. The atmospheric dynamics of Venus according to Doppler measurements by the Venera entry probes. In *Venus*, ed. DM Hunten, L Colin, TM Donahue, VI Moroz, pp. 766–78. Tucson: Univ. Ariz. Press
Khatuntsev IV, Patsaeva MV, Titov DV, Ignatiev NI, Turin AV, et al. 2013. Cloud level winds from the Venus Express Monitoring Camera imaging. *Icarus* 226:140–58
King-Hele DG. 1964. The rotational speed of the upper atmosphere, determined from changes in satellite orbits. *Planet. Space Sci.* 12:835–53
Kliore AJ, Patel IR. 1980. Vertical structure of the atmosphere of Venus from Pioneer Venus orbiter radio occultations. *J. Geophys. Res.* 85:7957–62
Kostiuk T, Fast KE, Livengood TA, Hewagama T, Goldstein J, et al. 2001. Direct measurements of winds on Titan. *Geophys. Res. Lett.* 28:2361–64
Kostiuk T, Hewagama T, Fast KE, Livengood TA, Annen J, et al. 2010. High spectral resolution infrared studies of Titan: winds, temperature, and composition. *Planet. Space Sci.* 58:1715–23

Kouyama T, Imamura T, Nakamura M, Satoh T, Futaana Y. 2013. Long-term variation in the cloud-tracked zonal velocities at the cloud top of Venus deduced from Venus Express VMC images. *J. Geophys. Res.* 118:37–46

Kraucunas I, Hartmann DL. 2005. Equatorial superrotation and the factors controlling the zonal-mean zonal winds in the tropical upper troposphere. *J. Atmos. Sci.* 62:371–89

Laraia AL, Schneider T. 2015. Superrotation in terrestrial atmospheres. *J. Atmos. Sci.* 72:4281–96

Lebonnois S, Burgalat J, Rannou P, Charnay B. 2012a. Titan Global Climate Model: new 3-dimensional version of the IPSL Titan GCM. *Icarus* 218:707–22

Lebonnois S, Covey C, Grossman A, Parish H, Schubert G, et al. 2012b. Angular momentum budget in General Circulation Models of superrotating atmospheres: a critical diagnostic. *J. Geophys. Res.* 117:E12004

Lebonnois S, Flasar FM, Tokano T, Newman CE. 2014. The general circulation of Titan's lower and middle atmosphere. In *Titan: Interior*, *Surface*, *Atmosphere and Space Environment*, ed. I Mueller-Wodarg, C Griffith, E Lellouch, T Cravens, pp. 122–57. New York: Cambridge Univ. Press

Lebonnois S, Hourdin F, Eymet V, Crespin A, Fournier R, Forget F. 2010. Superrotation of Venus' atmosphere analyzed with a full general circulation model. *J. Geophys. Res.* 115:E06006

Lebonnois S, Lee C, Yamamoto M, Dawson J, Lewis SR, et al. 2013. Models of Venus atmosphere. In *Towards Understanding the Climate of Venus: Application of Terrestrial Models to Our Sister Planet*, ed. L Bengtsson, RM Bonnet, D Grinspoon, S Koumoutsaris, S Lebonnois, D Titov, pp. 129–56. New York: Springer-Verlag

Lebonnois S, Sugimoto N, Gilli G. 2016. Wave analysis in the atmosphere of Venus below 100-km altitude, simulated by the LMD Venus GCM. *Icarus* 278:38–51

Lee C, Lewis SR, Read PL. 2005. A numerical model of the atmosphere of Venus. *Adv. Space Res.* 36:2142–45

Leovy CB. 1973. Rotation of the upper atmosphere of Venus. *J. Atmos. Sci.* 30:1218–20

Lewis SR, Dawson J, Lebonnois S, Yamamoto M. 2013. Modeling efforts. In *Towards Understanding the Climate of Venus: Application of Terrestrial Models to Our Sister Planet*, ed. L Bengtsson, RM Bonnet, D Grinspoon, S Koumoutsaris, S Lebonnois, D Titov, pp. 111–27. New York: Springer-Verlag

Lewis SR, Read PL. 2003. Equatorial jets in the dusty Martian atmosphere. *J. Geophys. Res.* 108:5034

Limaye SS. 1985. Venus atmospheric circulation: observations and implications of the thermal structure. *Adv. Space Res.* 5:51–62

Limaye SS, Suomi VE. 1981. Cloud motions on Venus: global structure and organization. *J. Atmos. Sci.* 38:1220–35

Linkin VM, Blamont JE, Lipatov AN, Devyatkin SI, Dyachkov AV, et al. 1986. Vertical thermal structure in the Venus atmosphere from provisional Vega 2 temperature and pressure data. *Sov. Astron. Lett.* 12:40–42

Livermore PW, Hollerbach R, Jackson A. 2013. Electromagnetically driven westward drift and inner-core superrotation in Earth's core. *PNAS* 110:15914–18

Longuet-Higgins MS. 1968. The eigenfunctions of Laplace's tidal equations over a sphere. *Philos. Trans. R. Soc. A* 262:511–607

Lora JM, Lunine JI, Russell JL. 2015. GCM simulations of Titan's middle and lower atmosphere and comparison to observations. *Icarus* 250:516–28

Lorenz RD, Stiles BW, Aharonson O, Lucas A, Hayes AG, et al. 2013. A global topographic map of Titan. *Icarus* 225:367–77

Louden T, Wheatley PJ. 2015. Spatially resolved eastward winds and rotation of HD189733b. *Astrophys. J. Lett.* 814:L24

Luz D, Civeit T, Courtin R, Lebreton JP, Gautier D, et al. 2005. Characterization of zonal winds in the stratosphere of Titan with UVES. *Icarus* 179:497–510

Machado P, Luz D, Widemann T, Lellouch E, Witasse O. 2012. Mapping zonal winds at Venus's cloud tops from ground-based Doppler velocimetry. *Icarus* 221:248–61

Machado P, Widemann T, Peralta J, Gonçalves R, Donati JF, Luz D. 2017. Venus cloud-tracked and Doppler velocimetry winds from CFHT/ESPaDOnS and Venus Express/VIRTIS in April 2014. *Icarus* 285:8–26

Mayr HG, Harris I. 1983. Quasi-axisymmetric circulation and superrotation in planetary atmospheres. *Astron. Astrophys.* 121:124–36

Mellor GL, Yamada T. 1982. Development of a turbulent closure model for geophysical fluid problems. *Rev. Geophys. Space Phys.* 20:851–75

Mendonça JM, Read PL. 2016. Exploring the Venus global super-rotation using a comprehensive general circulation model. *Planet. Space Sci.* 134:1–18
Mendonça JM, Read PL, Wilson CF, Lee C. 2015. A new, fast and flexible radiative transfer method for Venus general circulation models. *Planet. Space Sci.* 105:80–93
Mendonça JM, Read PL, Wilson CF, Lewis SR. 2012. Zonal winds at high latitudes on Venus: an improved application of cyclostrophic balance to Venus Express observations. *Icarus* 217:629–39
Merlis TM, Schneider T. 2010. Atmospheric dynamics of Earth-like tidally locked aquaplanets. *J. Adv. Model. Earth Sys.* 2:13
Mitchell JL, Ádámkovics M, Caballero R, Turtle EP. 2011. Locally enhanced precipitation organized by planetary-scale waves on Titan. *Nat. Geosci.* 4:589–92
Mitchell JL, Vallis GK. 2010. The transition to superrotation in terrestrial atmospheres. *J. Geophys. Res.* 115:E12008
Moreno R, Marten A, Hidayat T. 2005. Interferometric measurements of zonal winds on Titan. *Astron. Astrophys.* 437:319–28
Moroz VI, Zasova LV. 1997. VIRA-2: a review of inputs for updating the Venus International Reference Atmosphere. *Adv. Space Res.* 19:1191–201
Nakamura M, Imamura T, Ishii N, Abe T, Kawakatsu Y, et al. 2016. AKATSUKI returns to Venus. *Earth Planets Space* 68:75
Newman CE, Lee C, Lian Y, Richardson MI, Toigo AD. 2011. Stratospheric superrotation in the TitanWRF model. *Icarus* 213:636–54
Newman M, Leovy CB. 1992. Maintenance of strong rotational winds in Venus' middle atmosphere by thermal tides. *Science* 257:647–50
Pechmann JB, Ingersoll AP. 1984. Thermal tides in the atmosphere of Venus: comparison of model results with observations. *J. Atmos. Sci.* 41:3290–313
Peralta J, Hueso R, Sánchez-Lavega A, Piccioni G, Lanciano O, Drossart P. 2008. Characterization of mesoscale gravity waves in the upper and lower clouds of Venus from VEX-VIRTIS images. *J. Geophys. Res.* 113:E00B18
Peralta J, Sánchez-Lavega A, López-Valverde MA, Luz D, Machado P. 2015. Venus's major cloud feature as an equatorially trapped wave distorted by the wind. *Geophys. Res. Lett.* 42:705–11
Piccialli A, Titov DV, Grassi D, Khatuntsev I, Drossart P, et al. 2008. Cyclostrophic winds from the Visible and Infrared Thermal Imaging Spectrometer temperature sounding: a preliminary analysis. *J. Geophys. Res.* 113:E00B11
Pierrehumbert RT. 2011. A palette of climates for Gliese 581g. *Astrophys. J.* 726:L8
Plumb RA. 1977. Angular momentum advection by axisymmetric motions. *Q. J. R. Meteorol. Soc.* 103:479–85
Pollack JB, Young RE. 1975. Calculations of the radiative and dynamical state of the Venus atmosphere. *J. Atmos. Sci.* 32:1025–37
Read PL. 1986. Super-rotation and diffusion of axial angular momentum. II. A review of quasi-axisymmetric models of planetary atmospheres. *Q. J. R. Meteorol. Soc.* 112:253–72
Read PL. 2013. The dynamics and circulation of Venus atmosphere. In *Towards Understanding the Climate of Venus: Application of Terrestrial Models to Our Sister Planet*, ed. L Bengtsson, RM Bonnet, D Grinspoon, S Koumoutsaris, S Lebonnois, D Titov, pp. 77–110. New York: Springer-Verlag
Read PL, Lewis SR. 2004. *The Martian Climate Revisited*. Chichester, UK: Springer-Praxis
Rossby CG. 1947. On the distribution of angular velocity in gaseous envelopes under the influence of large-scale mixing processes. *Bull. Am. Meteorol. Soc.* 28:55–68
Rossow WB. 1983. A general circulation model of a Venus-like atmosphere. *J. Atmos. Sci.* 40:273–302
Rossow WB, Williams GP. 1979. Large-scale motion in the Venus stratosphere. *J. Atmos. Sci.* 36:1377–89
Sanchez-Lavega A, Hueso R, Piccioni G, Drossart P, Peralta J, et al. 2008. Variable winds on Venus mapped in three dimensions. *Geophys. Res. Lett.* 35:L13204
Sanchez-Lavega A, Lebonnois S, Imamura T, Read PL, Luz D. 2017. The atmospheric dynamics of Venus. *Space Sci. Rev.* 212:1541–616
Saravanan R. 1993. Equatorial superrotation and maintenance of the general circulation in two-level models. *J. Atmos. Sci.* 50:1211–27

Sardeshmukh PD, Hoskins BJ. 1988. The generation of global rotational flow by steady idealized tropical divergence. *J. Atmos. Sci.* 45:1228–51
Schneider EK. 1977. Axially symmetric steady state models of the basic state for instability and climate studies. Part II. Nonlinear calculations. *J. Atmos. Sci.* 34:280–96
Schneider T. 2006. The general circulation of the atmosphere. *Annu. Rev. Earth Planet. Sci.* 34:655–88
Schofield JT, Taylor FW. 1983. Measurements of the mean, solar-fixed temperature and cloud structure of the middle atmosphere of Venus. *Q. J. R. Meteorol. Soc.* 109:57–80
Seiff A, Kirk DB, Young RE, Blanchard RC, Findlay JT, et al. 1980. Measurements of thermal structure and thermal contrasts in the atmosphere of Venus and related dynamical observations: results from the four Pioneer Venus probes. *J. Geophys. Res.* 85:7903–33
Showman AP, Cho J, Menou K. 2010. Atmospheric circulation of extrasolar planets. In *Exoplanets*, ed. S Seager, pp. 471–516. Tucson: Univ. Ariz. Press
Sicardy B, Ferri F, Roques F, Lecacheux J, Pau S, et al. 1999. The structure of Titan's stratosphere from the 28 Sgr occultation. *Icarus* 142:357–90
Snellen IAG, de Kok RJ, de Mooij EJW, Albrecht S. 2010. The orbital motion, absolute mass and high-altitude winds of exoplanet HD 209458b. *Nature* 465:1049–51
Sobel AH, Nilsson J, Polvani LM. 2001. The weak temperature gradient approximation and balanced tropical moisture waves. *J. Atmos. Sci.* 58:3650–65
Sromovsky LA, Fry PM. 1993. Dynamics of Neptune's major cloud features. *Icarus* 105:110–41
Staniforth A, Thuburn J. 2012. Horizontal grids for global weather and climate prediction models: a review. *Q. J. R. Meteorol. Soc.* 138:1–26
Starr VP. 1968. *The Physics of Negative Viscosity Phenomena*. New York: McGraw-Hill
Suarez MJ, Duffy DG. 1992. Terrestrial super-rotation: a bifurcation of the general circulation. *J. Atmos. Sci.* 49:1541–54
Sugimoto N, Takagi M, Matsuda Y. 2014a. Baroclinic instability in the Venus atmosphere simulated by GCM. *J. Geophys. Res. Planets* 119:1950–68
Sugimoto N, Takagi M, Matsuda Y. 2014b. Waves in a Venus general circulation model. *Geophys. Res. Lett.* 41:7461–67
Takagi M, Matsuda Y. 2007. Effects of thermal tides on the Venus atmospheric superrotation. *J. Geophys. Res.* 112:D09112
Taylor FW, Beer R, Chahine MT, Diner DJ, Elson LS, et al. 1980. Structure and meteorology of the middle atmosphere of Venus: infrared remote sounding from the Pioneer Orbiter. *J. Geophys. Res.* 85:7963–8006
Tellmann S, Häusler B, Hinson DP, Tyler GL, Andert TP, et al. 2012. Small-scale temperature fluctuations seen by the VeRa Radio Science Experiment on Venus Express. *Icarus* 221:471–80
Tellmann S, Pätzold M, Hausler B, Bird MK, Tyler GL. 2009. Structure of the Venus neutral atmosphere as observed by the radio science experiment VeRa on Venus Express. *J. Geophys. Res.* 114:E00B36
Wang P, Mitchell JL. 2014. Planetary ageostrophic instability leads to superrotation. *Geophys. Res. Lett.* 41:4118–26
Widemann T, Lellouch E, Donati JF. 2008. Venus Doppler winds at cloud tops observed with ESPaDOnS at CFHT. *Planet. Space Sci.* 56:1320–34
Yamamoto M, Takahashi M. 2015. Dynamics of polar vortices at cloud top and base on Venus inferred from a general circulation model: case of a strong diurnal thermal tide. *Planet. Space Sci.* 113:109–19
Young RE, Pollack JB. 1977. A three-dimensional model of dynamical processes in the Venus atmosphere. *J. Atmos. Sci.* 34:1315–51
Young RE, Walterscheid RL, Schubert G, Pfister L, Houben H, Bindschadler DL. 1994. Characteristics of finite amplitude stationary gravity waves in the atmosphere of Venus. *J. Atmos. Sci.* 51:1857–75
Young RE, Walterscheid RL, Schubert G, Seiff A, Linkin VM, Lipatov AN. 1987. Characteristics of gravity waves generated by surface topography on Venus: comparison with the VEGA Balloon results. *J. Atmos. Sci.* 44:2628–39
Zalucha AM, Michaels TI. 2013. A 3D general circulation model for Pluto and Triton with fixed volatile abundance and simplified surface forcing. *Icarus* 223:819–31
Zasova LV, Ignatiev NI, Khatuntsev IA, Linkin V. 2007. Structure of the Venus atmosphere. *Planet. Space Sci.* 55:1712–28

Annual Review
of Earth and
Planetary Sciences
Volume 46, 2018

Contents

Errata

An online log of corrections to *Annual Review of Earth and Planetary Sciences* articles may be found at http://www.annualreviews.org/errata/earth